

Fault Diagnosis on a 330kV Power System Transmission Line Using Integrated S-Transform, Artificial Neural Network and Travelling Wave Techniques.

Ojukwu, A.C. *, Onuegbu, J.C., Abonyi, S.E and Ogbob, V.C.

Department of Electrical Engineering, Nnamdi Azikiwe University, Awka, Nigeria.

*Corresponding Author's E-mail: ojukwualbert@yahoo.com

Abstract

Due to the frequent and unpredictable occurrence of fault in our power transmission system, a need for the method intelligent enough to identify, categorize, and locate faults becomes imminent so as to ensure and guarantee an optimal reliability of the protection system of the transmission system/network. This paper presents an integral approach for fault diagnosis using a time-frequency (S-Transform) technique for fault detection, an Artificial Neural Network (ANN) called Pattern Recognition Algorithm for fault classification and a Travelling Wave technique for fault location on 47.39km Ajaokuta to Lokoja 330kV transmission line based on MATLAB/SIMULINK simulation and analysis. The S-Transform method employs a scalable and moving localizing Gaussian window to identify fault using the energy of the voltage and current signals, the chosen ANN classification network makes use of the pre-fault and fault voltages and current data to train the neural network to be able to classify fault and the Traveling wave approach uses the line voltage, current, propagation velocity, inductance, capacitance and length of line to find the fault distance. Various fault types were simulated on MATLAB/SIMULINK software and for each, the value of current magnitude of the energy signal were greater than the value of the voltage magnitude of the energy signal in accordance to conventional circuit theorem, a successful fault classification with a good performance and gradient value and the fault distance located along the transmission line.

Keywords: S-Transform, Pattern Recognition, Travelling Wave, Waveform and Signal.

1. Introduction

The transmission line is a crucial component of the electrical power system that transfers generated power to consumers. Transmission line can either be overhead or underground type depending on how they are installed. The overhead type of transmission line system seems to be quite the cheaper and effective means of transferring electrical power over a long distance. Transmission lines are one of the most vulnerable engineering systems due to their large length and considerable environmental exposure. Storms, rain, wind, and other natural disasters, as well as wildlife, birds, and even developing vegetation, all result in short circuits between the intermediate lines and the grounds. Supplying uninterrupted power to end user becomes a huge challenge due to this frequently occurring faults in the transmission line. Although these faults are unavoidable, it is imminent to accurately identify, categorize, and pinpoint fault distance. Relays quickly and accurately detect faults, allowing the faulty part to be isolated from the system. This is essential to protect equipment and maintain continuity of power to healthy parts of the system. Additionally, accurate fault classification also provides critical information about fault location, speeding up repair efforts thereby reducing system downtime (Moursalou, 2015; Luke and Erika, 2020).

Several studies have established several approaches for fault identification on a transmission line, which have been fully evaluated. Each of these studies emphasized the important discoveries, methodologies, and contributions made to the subject of fault analysis in power system engineering. Shafiullah, Abido and Al-Mohammed in "Advanced signal processing techniques (SPTs) for feature extraction", introduced the importance of SPTs in analyzing power system transients. They illustrated two advanced SPTs: the discrete wavelet transforms and the Stockwell transform. After the illustration of the targeted SPT, they presented a step-by-step feature extraction process from the recorded three-phase faulty current signals. S-transform was also used to extract useful features from the phasor measurement units (PMU) recorded current signals. The approach fetches the extracted features as inputs to the machine learning tools including the multilayer perception neural network, support vector machine and extreme learning machine to diagnose i.e., to detect, classify and locate the faults. (Shafiullah, 2022). Additionally, in "S-transform based fault detection algorithm for enhancing distance protection performance," Jose, Marjan, David, Sadegh, and Vladimir (2021) proposed a fault detection algorithm based on the Fast Discrete Stockwell Transform. This algorithm can address issues found during fault detection and improve the functionality of the current distance protection during fault occurrence in systems with high penetration of power electronics-based generators.

In Ravi, Ebha, Anamika, and Thoke's article from 2014, "fault classification of phase-to-phase fault in six phase transmission line using Haar wavelet and ANN," They discovered that the two approaches depended on the standard deviation of the estimated coefficients of voltage and current obtained for all potential line-to-line faults from a single side only. It was shown that both approaches were accurate in identifying all fifteen types of line faults for a six-phase transmission line. These two approaches work for all sorts of line-to-line fault resistance, therefore changing the inception angle or even the resistance fault will not impact the classification result. Ahmed Sabri Altaie (2015) focuses on a novel way to detect, classify, and localize transmission line faults in "Design of a new digital relay for transmission line fault detection, classification, and localization based on new composite relay and artificial neural network approach." First, the novel composite relay (CR) was employed to detect failures of any kind, including series faults. Second, the Feed Forward Artificial Neural Network (FFANN) was used to classify faults and determine the most effective way to use it. The three-phase series compensated network in MATLAB/SIMULINK served as the data source.

Lastly, the type of fault localization to use was selected using FFANN in combination with a digital controller. In "Accurate two-terminal transmission line fault location using travelling waves," Lopes, Dantas, Silva, and Costa (2017) introduced a fault localization method based on two-terminal TW approach. Data synchronization of the line parameter is not required since this approach relies on the time delay between the initial incident wave and the subsequent reflection from the fault spot at both ends of the line. Another TW-based protection algorithm for parallel transmission lines is described by Hasheminejad, Seifossadat, Razaz, and Joorabian (2016) in "Traveling-wave-based protection of parallel transmission lines using Teager energy operator and fuzzy systems," which makes use of Karenbahe's phase to modal transform and Teagar energy operator. It proved to be quite successful as a high accuracy of 0.9% for the greatest error and 0.15% for the least error was reached.

Despite the numerous and significant discovery in the subject of fault analyses, most researchers have failed to integrate some of the techniques together to achieve a more efficient model. This paper presents an integral approach for fault diagnosis using S-Transform technique based on a moving and scalable localizing Gaussian window for fault detection, Pattern Recognition Algorithm of ANN using the pre-fault, fault voltage and current of the transmission line were used as inputs of the ANN network selected for fault classification and Traveling Wave technique which uses the voltage and current coming from the transmission line as well as distance of the line, the propagation velocity, inductance of the line, capacitance of the line and change in the time that the fault occurs for fault location. The various techniques employed for the diagnosis were discussed in details. The 47.39km Ajaokuta to Lokoja 330kV transmission line was extracted from the MATLAB/SIMULINK Nigeria 58 bus system model and used as a case study to simulated the various fault conditions (phase to ground, double phase, phase to phase and three phase fault) which acts an input to the S-Transform model, Patten Recognition model and Travelling wave model in MATLAB/SIMULINK. The results from the diagnosis of each fault case were also discussed.

2.0 Material and methods

The methodology employed in carrying out this study is presented. A three-method (ANN, S-Transform, and Traveling wave) case study approach was used. The 47.39km Ajaokuta-Lokoja 330kV transmission line was extracted and modelled from the Nigerian 58-bus system in MATLAB/SIMULINK. The S-Transform equation was modelled using MATLAB/SIMULINK blocks. The pre-fault and fault values of the voltage and current was used as an input to the ANN model to train the pattern recognition algorithm against the target truth table of table 3. The traveling wave equation was also modelled using the MATLAB/SIMULINK blocks. The integral model was simulated at pre-fault and various fault conditions. At various fault conditions, the magnitude of the energy of the voltage and current signal were used to detect whether fault occurred, the ANN model performance and gradient were used to check for successful classification and the estimated distance at which the fault occurred was displayed in the travelling wave model. The block diagram in figure 1 represents the methodological procedure for this research.

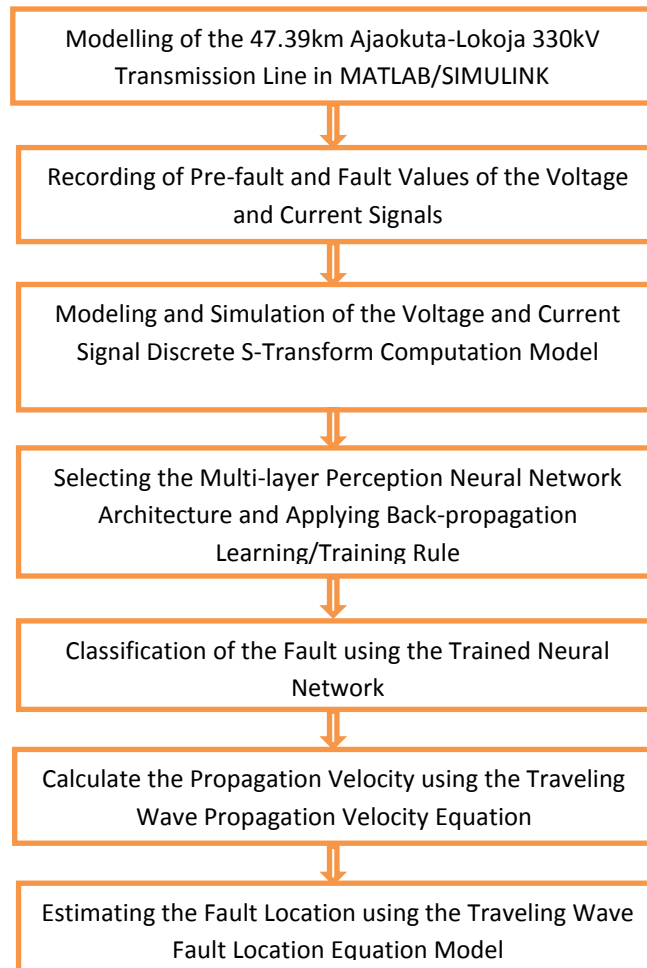


Figure 1: A Block Diagram Illustrating the Research's Methodology.

The input phase voltage (V_a, V_b and V_c) and phase current (I_a, I_b and I_c) are the input parameters to the power system network model gotten from the 47.39km Ajaokuta-Lokoja 330kV transmission line of the 58-Bus power system network as shown in Table 1.

Table 1: Pre-fault Voltage and Pre-fault Current Parameter (Input Data) Obtained from the 47.39km Ajaokuta-Lokoja 330kV Transmission Line of the 58-Bus Power System Network

Pre-Fault Voltage and Current Parameter in pu					
V_a	V_b	V_c	I_a	I_b	I_c
0.330226	-0.66065	0.330427	-0.31355	0.158394	1.55E-01
0.339173	-0.66057	0.3214	-0.31354	0.154124	0.159412
0.348036	-0.66033	0.312294	-0.31345	0.149817	0.163635
0.356813	-0.65992	0.303111	-0.31329	0.145473	0.167817
0.365503	-0.65936	0.293853	-0.31305	0.141094	0.171957
0.374102	-0.65863	0.284523	-0.31273	0.136678	0.176055
0.382609	-0.65773	0.275122	-0.31234	0.132229	0.18011
0.391022	-0.65668	0.265654	-0.31187	0.127747	0.184119
0.399338	-0.65546	0.25612	-0.31132	0.123234	0.188084
0.407555	-0.65408	0.246523	-0.31069	0.11869	0.192002
0.415672	-0.65254	0.236865	-0.30999	0.114117	0.195872
0.423687	-0.65084	0.227148	-0.30921	0.109515	0.199694
0.431597	-0.64897	0.217376	-0.30835	0.104886	0.203466
0.4394	-0.64695	0.20755	-0.30742	0.100231	0.207188
0.447095	-0.64477	0.197672	-0.30641	0.09555	0.210857
0.454679	-0.64243	0.187746	-0.30532	0.090846	0.214475
0.462152	-0.63993	0.177774	-0.30416	0.086121	0.218041

The fault voltage (V_{af} , V_{bf} and V_{cf}) and fault current (I_{af} , I_{bf} and I_{cf}) are the output parameters of the modelled system as shown in the Table 2 indicating the different fault conditions simulated.

Table 2: Fault Voltage and Fault Current Parameter (Output Data) of the Different Fault Simulation Obtained from the 47.39km Ajaokuta-Lokoja 330kV Transmission Line of the 58-Bus Power System Network

Fault Voltage and Current Parameter in pu						
Condition	V_{af}	V_{bf}	V_{cf}	I_{af}	I_{bf}	I_{cf}
No Fault	0.330226	-0.66065	0.330427	-0.31355	0.158394	1.55E-01
A – G	0.3511	-0.6603	0.3091	-1.721	0.3015	0.2968
B – G	0.3801	-0.7106	0.3305	-0.1471	1.318	0.3172
C – G	3.31E-01	-0.6185	2.88E-01	0.1576	6.36E-01	-0.7676
A – B	0.2419	-0.617	0.3752	2.296	-2.447	0.1505
B – C	0.4102	-0.8198	0.4095	-0.3147	-0.5994	0.9139
C – A	0.3331	-0.6586	0.3256	2.417	0.1653	-2.583
AB – G	0.3324	-0.7272	0.3949	-0.4051	0.8533	2.7
BC – G	0.2724	-0.6411	0.3687	2.08E+00	-0.554	-0.02734
CA – G	0.4059	-0.7511	0.3452	-0.6231	-0.6858	0.3115
A – B – C	0.2425	-0.7084	0.4659	3.1	-1.644	-1.456

2.1 Modeling of the S-Transform Equation for Detection of Fault Using MATLAB/SIMULINK

Stockwell et al. (1996) presented the S-transform in "Localization of the Complex Spectrum: The S-transform," which is a variation that shows some of the desirable properties that are lacking in the continuous wavelet transform like the ability to detect the disturbance correctly in the presence of noise. While keeping its link with the Fourier spectrum, the S-transform provides a unique frequency dependent resolution.

S-Transform of a basic continuous signal (voltage and current signal) $h(t)$ of a transmission line is defined by the following equation;

$$S(\tau, f) = \int_{-\infty}^{\infty} h(t) w(f, \tau - t) e^{(-2\pi i f t)} dt \quad (1)$$

But,

$$w(f, \tau) = \frac{|F|}{\sqrt{2\pi}} e^{-\left(\frac{t^2}{2\alpha^2}\right)} \tag{2}$$

Where equation (2) is called the Gaussian modulating function

$$S(\tau, f) = \int_{-\infty}^{\infty} h(t) \left\{ \frac{|f|}{\alpha\sqrt{2\pi}} \right\} \cdot e^{\left(\frac{-f^2(\tau-t)^2}{2\alpha^2}\right)} \cdot e^{(-2\pi ift)} dt \tag{3}$$

Combining equation (1) and (2), we obtain equation (3)

Where f is the frequency in hertz, t is the time in seconds, and τ is the time location in seconds also known as the parameter determining the position of the Gaussian window on the t -axis and α is the standard deviation, which functions as a control factor for the transform's time and frequency resolution. Lower α values correspond to lower frequency and better temporal resolution, and vice versa.

A reasonable value for α falls between 0.2 and 1.

Equation (4) provides the DST expression while taking the discrete form of the continuous S-Transform into consideration.

$$S(j, n) = \sum_{m=0}^{N-1} H(m + n) \cdot e^{\left(\frac{-2\pi^2 m^2 \alpha^2}{n^2}\right)} \cdot e^{(i2\pi mj)} \tag{4}$$

Where, $j = 1 \dots N-1$, $n = 0, 1 \dots N-1$. But the time samples and frequency step are indicated by j and n respectively.

Next, the S-Transform yields the signal's energy E , which is as

$$E = \{abs(S(j, n_1))\}^2 \tag{5}$$

The energy signal that you acquire from the S-Transform is used for the identification and classification of the transmission line fault (Anazia, Ogbob and Anionovo, 2020, Iwuamadi, Ezechukwu and Ogbob, 2022).

The DST S-Transform equation from (4) is modelled in MATLAB/SIMULINK for the voltage and current signal and the result model is shown in Figure 2 and 3.

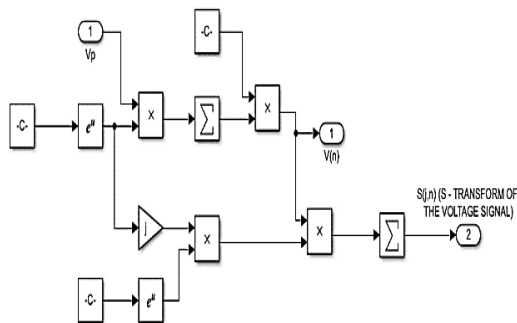


Figure 2: The S-Transform Discrete Model Voltage Signal.

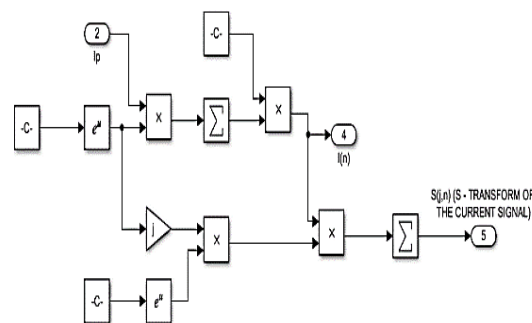


Figure 3: The S-Transform Discrete Model for Current Signal.

The discrete energy signal of voltage and current is the signal that depicts the magnitude, severity, and frequency of line faults. The Simulink model is displayed below.

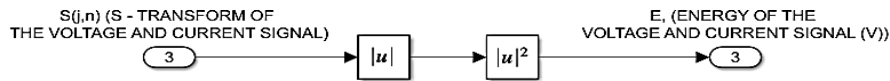


Figure 4: The Voltage and Current Discrete S-Transform Energy Signal Simulink Model.

Conventional theories of networks or circuits state that when a fault arises in an electrical circuit, the magnitude of the voltage drops and the magnitude of the current rises. Consequently, the voltage energy signal's amplitude can only exceed the current energy signal's size in the absence of fault in the network. It is expected that the voltage energy signal would be less than the current energy signal when a fault occurs in the network. If, following fault simulations, the voltage energy signal output is larger than the current energy signal output, the energy equation of (5) is not true (Iwuamadi et al., 2022).

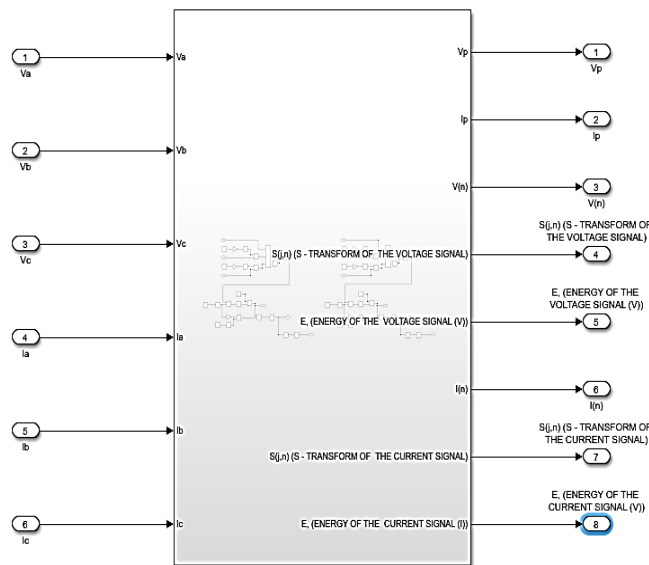


Figure 5: The Discrete S-Transform Model for the Voltage and Current Signal: A Comprehensive MATLAB/SIMULINK Subsystem.

The MATLAB/SIMULINK subsystem model is used to compute the discrete values of the voltage and current during pre-fault and fault conditions, as well as the energy models for the voltage and current signal and the S-Transform fault detection model, as shown in Figure 6. The output of the MATLAB/SIMULINK voltage-current measurement block is linked to the inputs of the S-Transform fault detection model to extract the phase voltage and current signals, which are then evaluated using the mathematical model. The outcome is provided to demonstrate whether there is a fault or not.

2.2 Modeling of the Fault Classification Technique Based on Pattern Recognition Algorithm of Artificial Neural Network (ANN) Using MATLAB/SIMULINK

According to Ogboh, Nwangugu and Anyalebechi (2019) in “Fault detection on power system transmission line using artificial neural network (A comparative case study of Onitsha-Awka-Enugu transmission line)”, the mapping process of a function \emptyset that characterizes the input-output ANN operating technique is given below.

$$y = \emptyset x \tag{6}$$

where \emptyset is the neural network's mapping function; Input vector: x ; Output vector: y .

The Neural Network's Learning Process

To achieve the intended design goal, the learning algorithm adjusts the synaptic weights in the network to match the aim. After the neural network has been trained, the output is generalized using a mathematical procedure. The neural network has the ability to produce logical results for inputs that were not present during training, this is referred to as generalization. The following fundamental attributes of the neural network are significant to this work:

- **Input-Output Mapping:** For both real and simulation-based situations, the input signals to the network are the pre-fault and fault voltage and fault current phase values. The weights are adjusted to reduce the discrepancy between the desired and network outputs. It is necessary to be aware of the target values representing the desired output so as to use the supervised learning. The network is then continuously trained until there is no significance weight change which is known as a converging point.
- **Non-linearity:** Each non-linear component is represented by a neuron. The group of neurons makes up the neural network also known as a non-linear system.
- **Adaptively:** Once selected, the artificial neural network may be swiftly retrained to accommodate minor changes in the environment while being trained for a specific function (input-output pairs) in that environment.

Selecting the Proper Network

The ANN pattern recognition algorithm makes it feasible to differentiate between electrical power systems that are malfunctioning and those that are functioning normally by identifying which phase is experiencing a fault among the three-phase system.

The pre-fault and fault values of the voltage and current of the corresponding line are determined by the different fault types. The neural network is utilized for fault classification based on the patterns of the pre-fault and fault voltage and current values obtained from the transmission line at one point. The neural network's input (6) consists of the three phases' voltages and currents which is used to train the network. The types of faults make up the four outputs of the neural network (Ogboh, Obute and Eleanya, 2019, Majid, Sanjeer and Rajveer, 2015).

Table 3: The Truth Table of Back Propagation Neural Network for Fault Classification

Fault Condition	Network Outputs			
	A	B	C	G
No Fault	1	1	1	1
A – G	1	0	0	1
B – G	0	1	0	1
C – G	0	0	1	1
A – B	1	1	0	0
B – C	0	1	1	0
C – A	1	0	1	0
A – B – G	1	1	0	1
B – C – G	0	1	1	1
C – A – G	1	0	1	1
A – B – C	1	1	1	0

Using the simulated and real data for fault classification network, the above truth table (table 3) gives the desired output of the network. The classification of the fault type occurs immediately the fault happened. The learning strategy used is the back propagation (BP) algorithm. The process of changing the weights and biases of the network to train it to do a particular job is known as the learning rule or training algorithm. So therefore, the back propagation learning rule or training algorithm is used to train the fault classification multi-layer perception neural network.

According to Tables 1 and 2, the neural network with six neurons in the input layer, one hidden layer, ten hidden neurons, and four neurons in the output layer, or 6-10-4, achieved satisfactory performance among the back-propagation networks with various combinations of hidden layers and different numbers of neurons in each hidden layer that were analyzed. The training set has a total of 1001 input and output patterns (1000 for each of the ten fault types), with six inputs and one output in each input output combination.

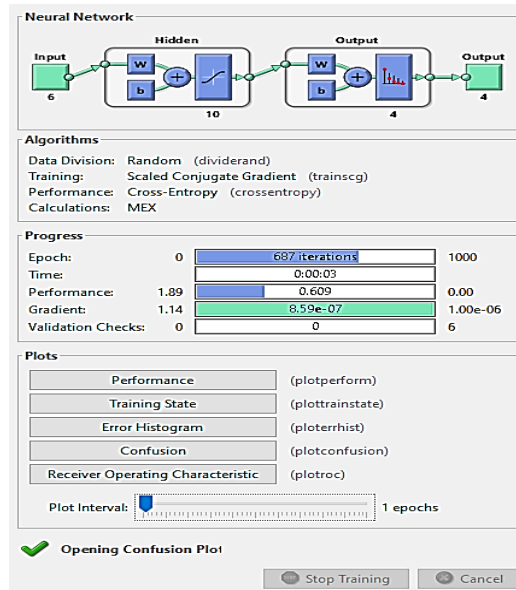


Figure 6: The Classification Network ANN Training Procedure.

Figure 6 depicts the ANN training process for the chosen classification network. It displays the gradient at 8.59×10^{-7} , the number of iterations (687), and the best validation performance of the network was 0.609 at 687 epochs. Since the network is fitted, and the training, testing, and validation curves all have comparable features, indicating effective training and a strong performance.

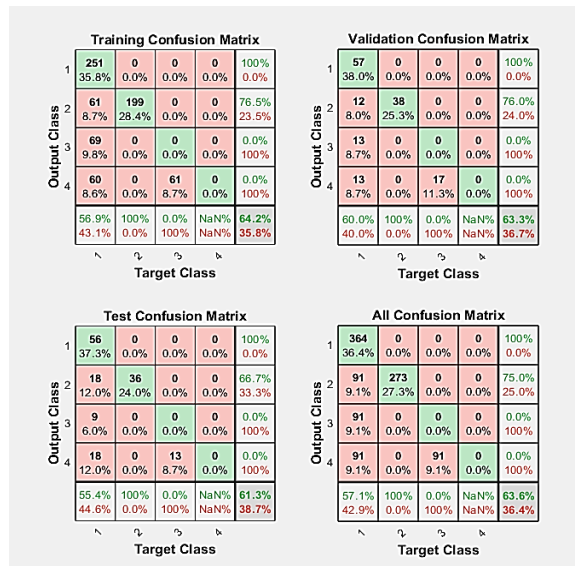


Figure 7: The Classification Network Confusion Matrix.

The training, testing and validation stages has its confusion matrix presented in figure 7. Another way to evaluate the neural network's performance is by plotting the confusion matrices of the fault's types. The number of instances the neural network correctly classified are indicated by the diagonal green cells while the incorrect classifications are indicated by the off-diagonal red cells. The last blue cell in each matrix represents the overall proportion of properly categorized instances in green, and vice versa for ash. The trained neural network's 63.8 percent effectiveness in determining the kind of defect is displayed in figure 7. In conclusion, the neural network can distinguish between each of the 10 various kinds of transmission line faults.

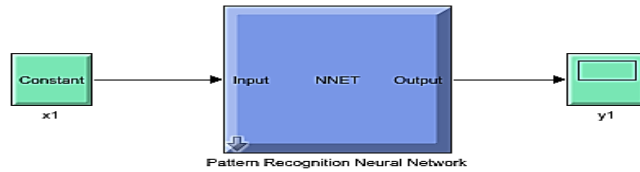


Figure 8: The Fault Classification Simulink Discrete Pattern Recognition ANN Subsystem Model.

The classification model was extracted into a Simulink system model for easy integration as seen in figure 8.

2.3 Modelling of the Fault Location Based on Traveling Wave Technique Using MATLAB/SIMULINK

The reliability of power system operation depends on its ability to detect, locate, isolate and repair fault quickly as they occur. The voltage value at the point of failure drops dramatically as a fault occur on the transmission line. The sudden change generates a high frequency electromagnetic impulse known as a Travelling Wave (TW). The travelling wave accelerates away from the fault in both directions at nearly the speed of light. The fault is subsequently located and detected using the filtered signal (Raza, Benrabah, Alquthami and Akmal, 2020).

A traveling wave is used in some of the most popular and trustworthy fault techniques; the two-ended idea is illustrated here.

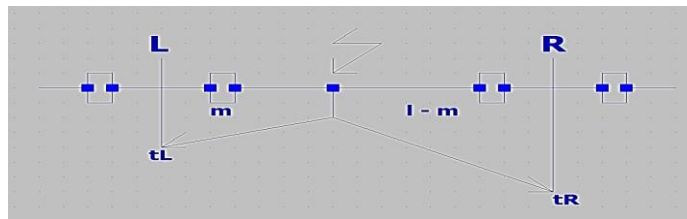


Figure 9: Two Ended Fault Locations Depending on When the First Arrivals Happened.

Figure 9 illustrates the two-end fault location idea using traveling waves. It displays the location of the fault, and the traveling wave components that are reflected back to both the local and distant ends and the length of the line.

The fault location m is determined by comparing the arrival timing of the traveling waves at both ends of the line.

$$m = \frac{[l + (t_L - t_R)v]}{2} \quad (7)$$

where the transmission line length is l ; local end arrival time is t_L ; remote end arrival time is t_R and the velocity of propagation is v .

The propagation velocity is given as in equation 8

$$v = \sqrt{\frac{1}{\left(\frac{V^2 C}{l}\right) \times \left(\frac{l^2 L}{V^2}\right)}} \quad (8)$$

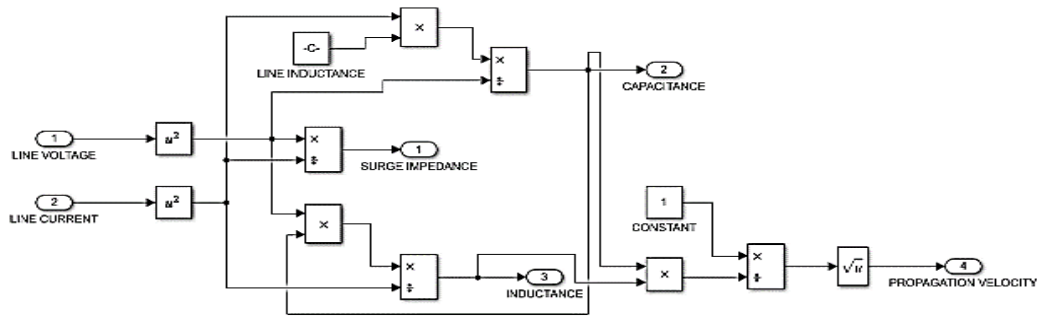


Figure 10: The Propagation Velocity of the Traveling Wave Equation Simulink Model

Modelling the propagation velocity of the traveling wave equation of (8) in MATLAB/SIMULINK gives the Simulink model in Figure 10.

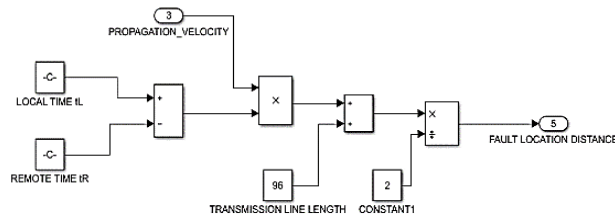


Figure 11: The Simulink Traveling Wave Fault Location Equation Model.

The MATLAB/SIMULINK model for the fault location equation model as in equation (7) is shown in Figure 11.

After replacing the propagation velocity, the fault distance (m) may be computed using the formula below: (John, Anionovo, and Obi, 2020)

$$m = \frac{l + (tL - tR) \sqrt{\frac{1}{\left(\frac{V^2 C}{T}\right) \times \left(\frac{l^2 L}{V^2}\right)}}}{2} \tag{9}$$

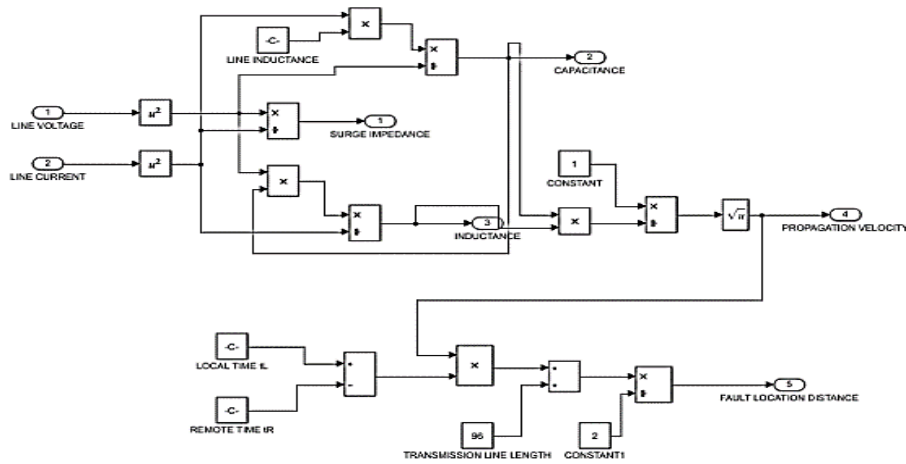


Figure 12: The Simulink Traveling Wave Fault Location Equation Model with Propagation Velocity Equation.

The Simulink model for the travelling wave fault localization equation is displayed in Figure 12, and it uses the propagation velocity equation to determine the fault's distance from the source.

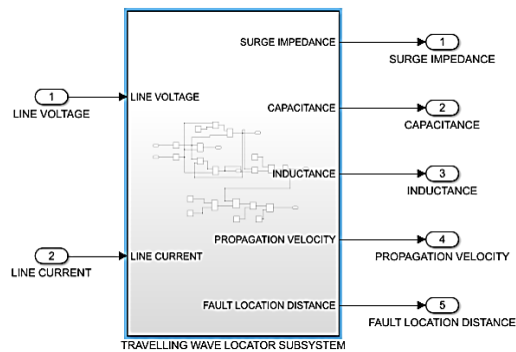


Figure 13: The Simulink Subsystem Traveling Wave Fault Location Model.

The MATLAB/SIMULINK subsystem model as seen in Figure 13 is used for the location of the distance at which the fault occurred from the source on the transmission line.

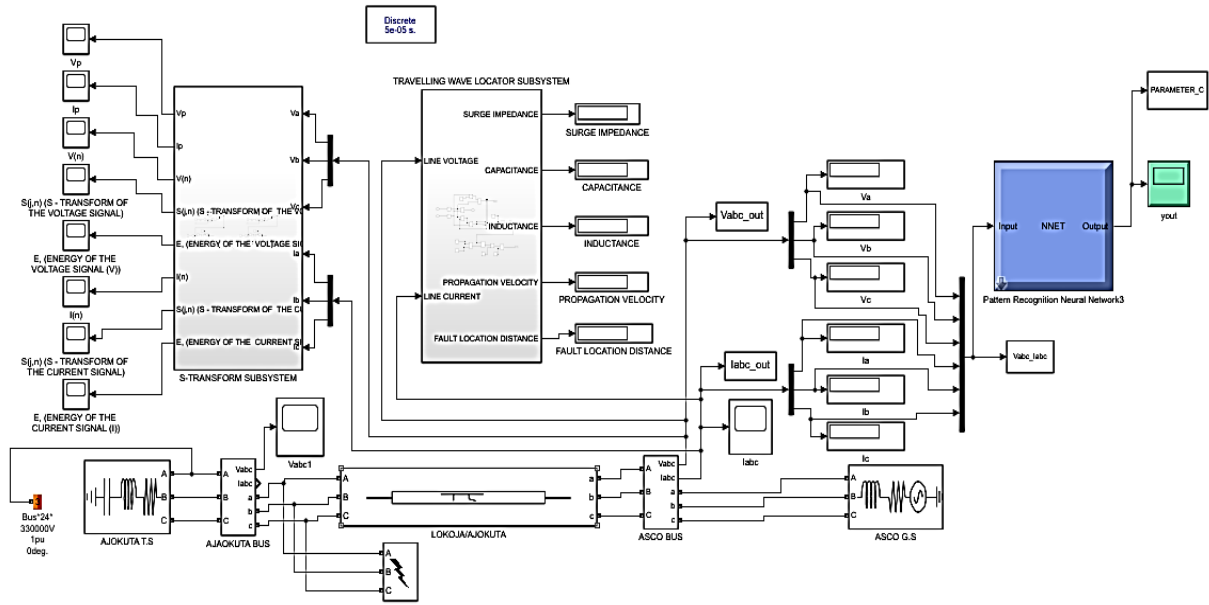


Figure 14: The MATLAB/SIMULINK Model Used for the Fault Diagnosis of the 330 kV Ajaokuta to Lokoja 47.39km Transmission Line Network using S-Transform, Pattern Recognition and Travelling Wave Techniques.

3.0 Results and Discussions

The results covered the finding from the fault diagnosis of the Nigerian 58-Bus network using a case study of the 47.39km Ajaokuta-Lokoja 330kV power transmission line. The outcomes were obtained using the several approaches that this study described. The following conclusions were reached as a result of simulating the Simulink model for the fault diagnostics for the different fault conditions.

i. At Pre-fault Condition

Figure 15 depicts the pre-fault voltage waveform of the system after modeling it with no fault. When there is no fault in the system, the three-phase voltage waveform moves in a uniform sinusoidal shape. The magnitude of the three-phase gaussian window width looks to be 0.65pu. Figure 16 depicts the pre-fault current wave of the system under consideration. Because there is no fault current in the system, the magnitude of the current is relatively the same for each phase at 0.3pu less than the value of the voltage at 0.65pu.

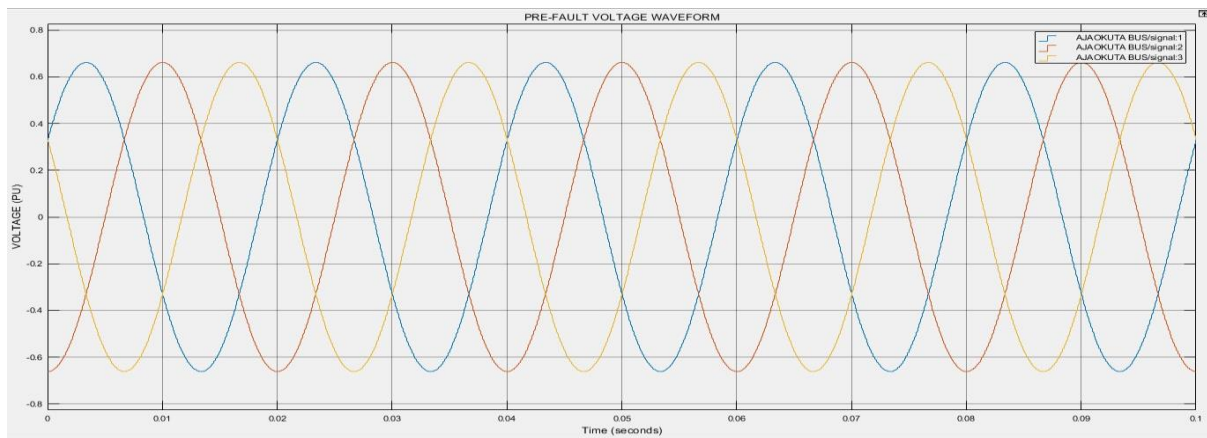


Figure 15: Pre-fault Voltage Waveform for the System Modelled

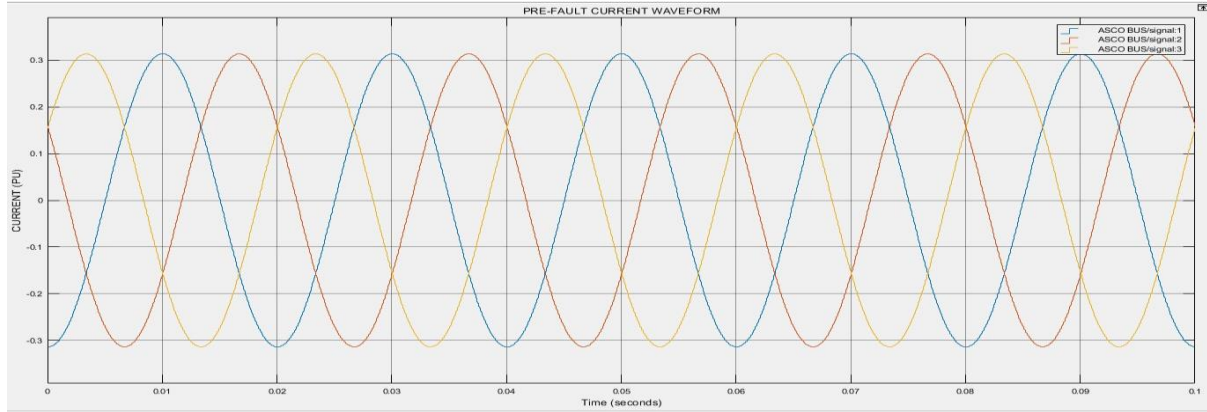


Figure 16: Pre-fault Current Waveform for the System Modelled.

Figure 17 depicts the energy of the voltage signal in the pre-fault situation. The magnitude of the voltage energy signal obtained from the S-transform model is $1.6947 \times 10^{27} J$, with a constant gaussian waveform throughout the plane. Figure 18 shows that the energy of the current signal obtained from the S-transform model is $1.2725 \times 10^{26} J$. Since there is no failure in the system, the magnitude of the energy of the voltage signal at $1.6947 \times 10^{27} J$ is larger than that of the energy of the current signal.

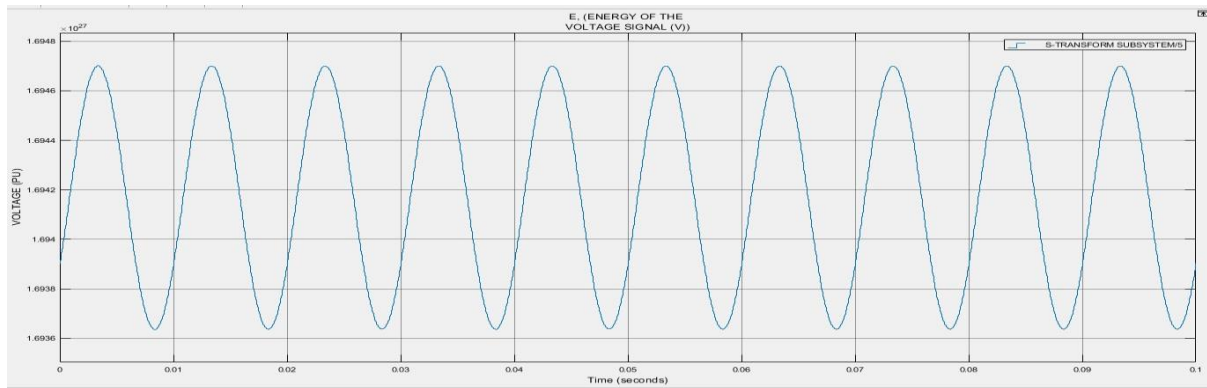


Figure 17: The Voltage Signal Energy Waveform during Pre-fault Condition.

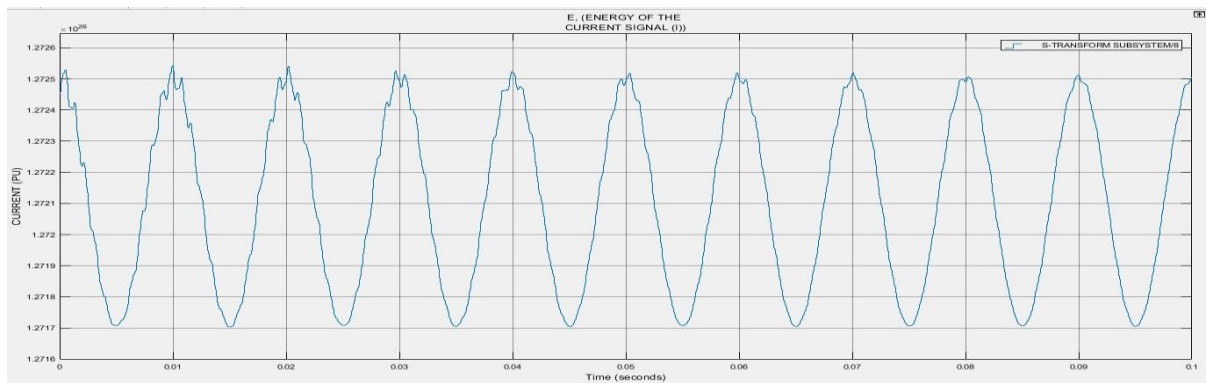


Figure 18: The Current Signal Energy Waveform during Pre-fault Condition.

Table 4: The Result Obtained at No Fault Condition

S/N	PARAMETER	MAGNITUDE (PU)
1	Voltage (V)	0.65

2	Current (I)	0.3
3	Energy of the voltage signal E_j (J)	1.6947×10^{27}
4	Energy of the current signal E_j (J)	1.2725×10^{26}

ii. At Single Phase to Ground Fault

The following data were obtained when a single phase to ground fault was simulated on the system, say on phase A, B, or C, at a time of 17msecs and persisted until it was cleared at 85msecs, which lasted roughly 68msecs.

During failure simulation, a spike was seen in the defective phase. The magnitude of the current in the defective phase grew to around 40pu for the single phase to ground, while the current in the remaining healthy phases remained unchanged. After the fault is resolved, the amplitude of the defective phase's current becomes uniform with the size of the remaining healthy phases' current. Figures 20 shows the current waveform.

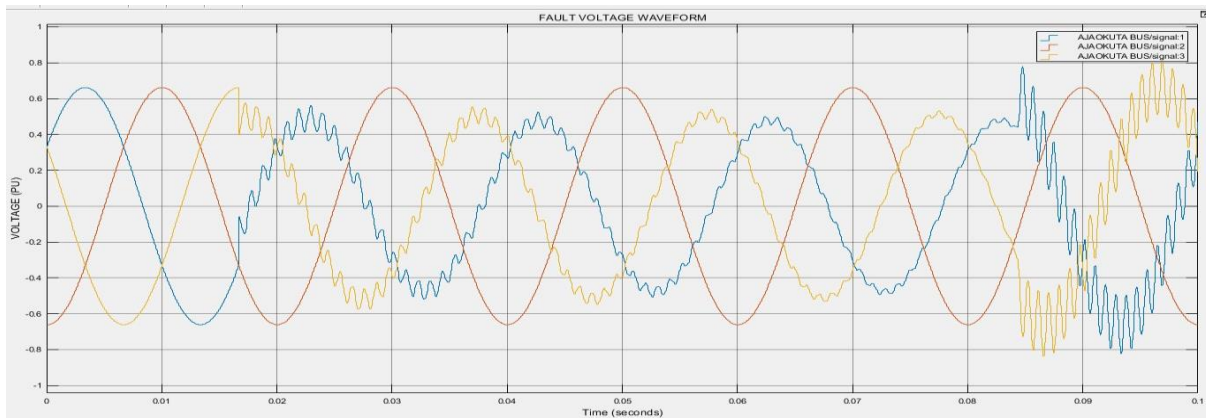


Figure 19: Single Phase to Ground Fault Voltage Waveform for the System Modelled.

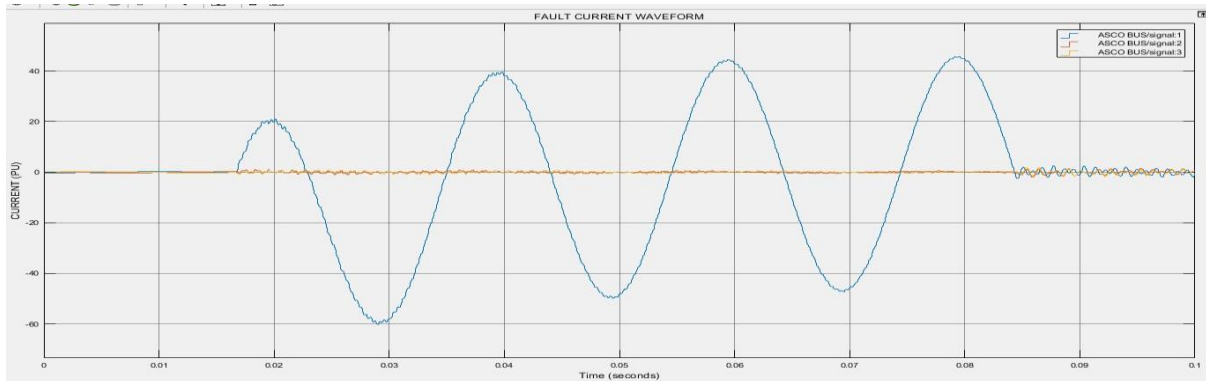


Figure 20: Single Phase to Ground Fault Current Waveform for the System Modelled.

Furthermore, the magnitude of the voltage energy signal from the S-Transform model in Figure 21 gets distorted at $1.7 \times 10^{27} J$ during the fault condition, which is now smaller than the magnitude of the current energy signal in Figure 22 at $2.0 \times 10^{30} J$. When the fault occurs at 17msecs, the current energy signal magnitude spikes to $2.0 \times 10^{30} J$ and is recovered once the fault is cleared at 85msecs.

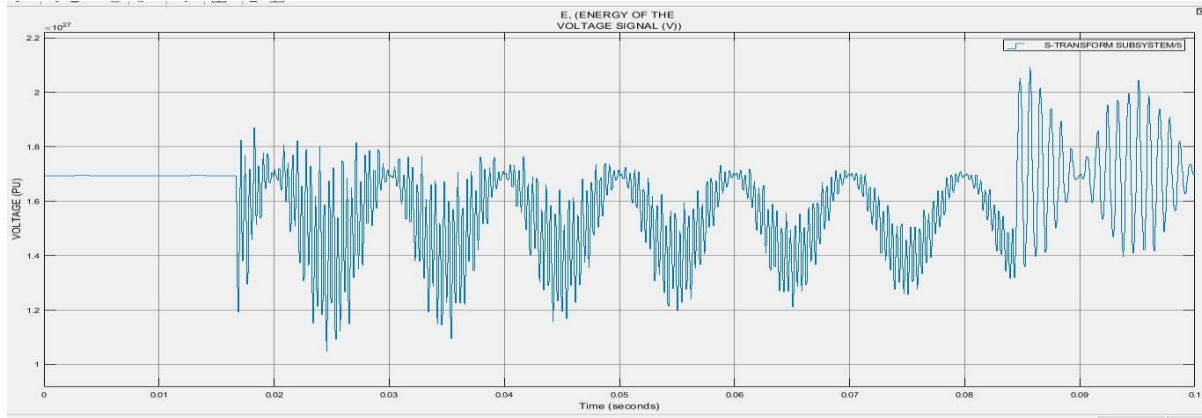


Figure 21: The Voltage Signal Energy Waveform during Single Phase to Ground Fault Condition

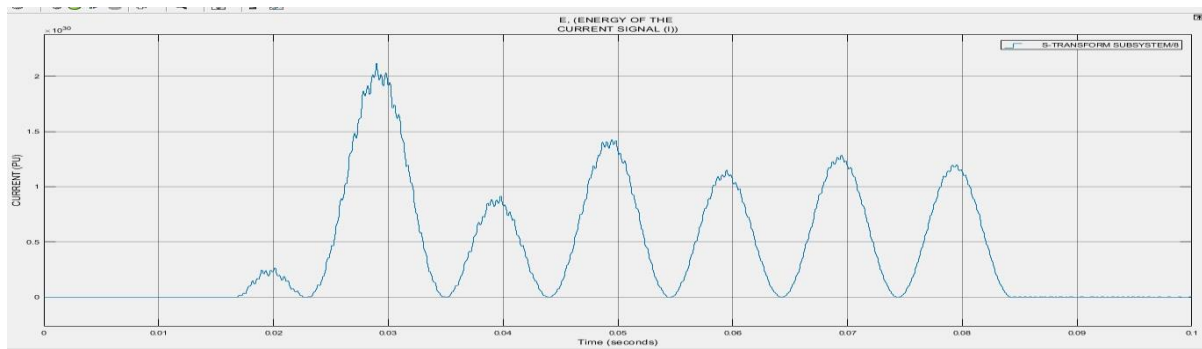


Figure 22: The Current Signal Energy Waveform during Single Phase to Ground Fault Condition.

Figure 23 depicts the fault classification back propagation ANN training approach chosen for the phase to ground (A-G, B-G, or C-G) fault. It displays the number of iterations (111), the network's performance (0.0385, which is good) and the gradient (which is 0.00184).

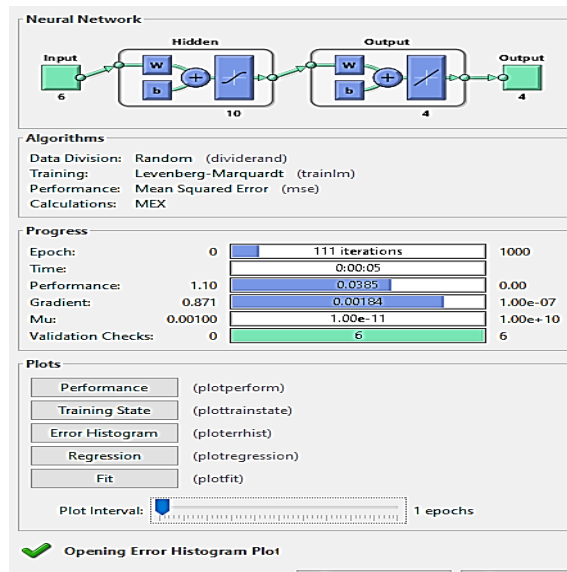


Figure 23: The Fault Classification BP ANN Training Procedure Selected for Single Phase to Ground Fault.

The distance at which the phase to ground fault occurred is locate at 44.03km gotten from the output of the traveling wave model.

Table 5: The Result Obtained at Phase to Ground Fault Condition

S/N	PARAMETER	MAGNITUDE (PU)
1	Voltage (V)	0.4
2	Current (I)	40
3	Energy of the voltage signal $E_j(J)$	1.7×10^{27}
4	Energy of the current signal $E_j(J)$	2.0×10^{30}
5	Mean Square Error (MSE)	0.0385
6	Gradient & Validation	0.00184
7	Fault Distance in km	44.03

iii. At Phase-to-Phase Fault Condition

The following findings were obtained when a phase-to-phase fault was simulated on the system, at a time of 17msecs and persisted until it was cleared at 94msecs, which lasted roughly 77msecs.

The current waveform reveals that once the fault arose, the faulty phase current magnitudes climbed to 120pu and persisted in this manner until the fault was cleared up. It was discovered that at the healthy phase, the amplitude of the current passing through it did not vary during the fault period. After the fault is resolved, the amplitude of the current in the faulty phases becomes uniform with the size of the current in the remaining healthy phase. Figures 25 shows the current waveform.

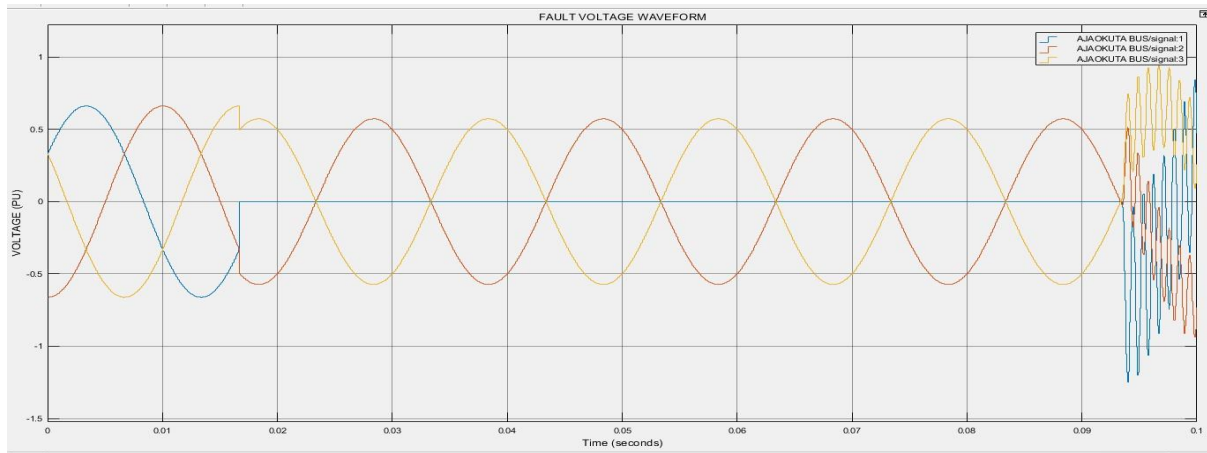


Figure 24: Phase to Phase Fault Voltage Waveform for the System Modelled.

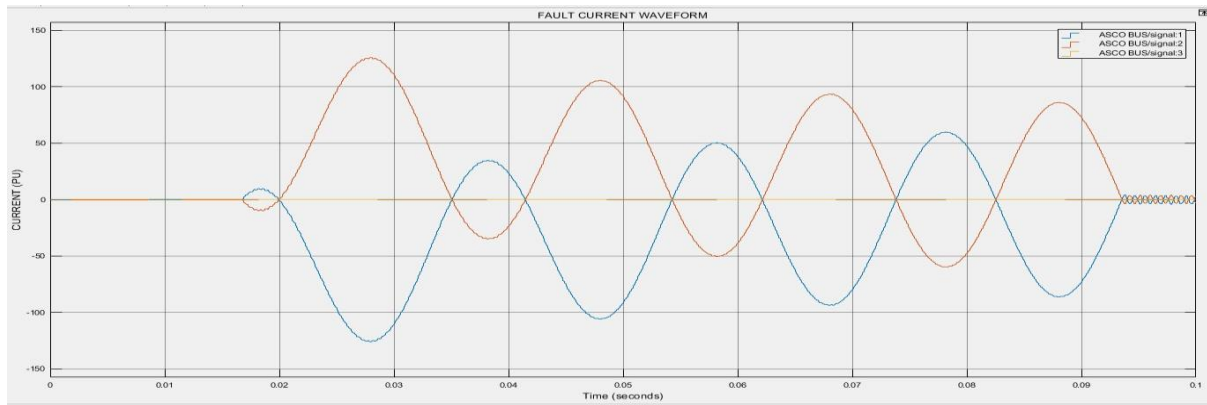


Figure 25: Phase to Phase Fault Current Waveform for the System Modelled.

Furthermore, the magnitude of the voltage energy signal from the S-Transform model in Figure 26 gets distorted at $1.7 \times 10^{27} J$ during the fault condition, which is now smaller than the size of the current energy signal in Figure 27 at $2.7 \times 10^{31} J$. When the fault occurs at 17msecs, the current energy signal magnitude spikes to $2.7 \times 10^{31} J$ and is recovered once the fault is cleared at 94msecs.

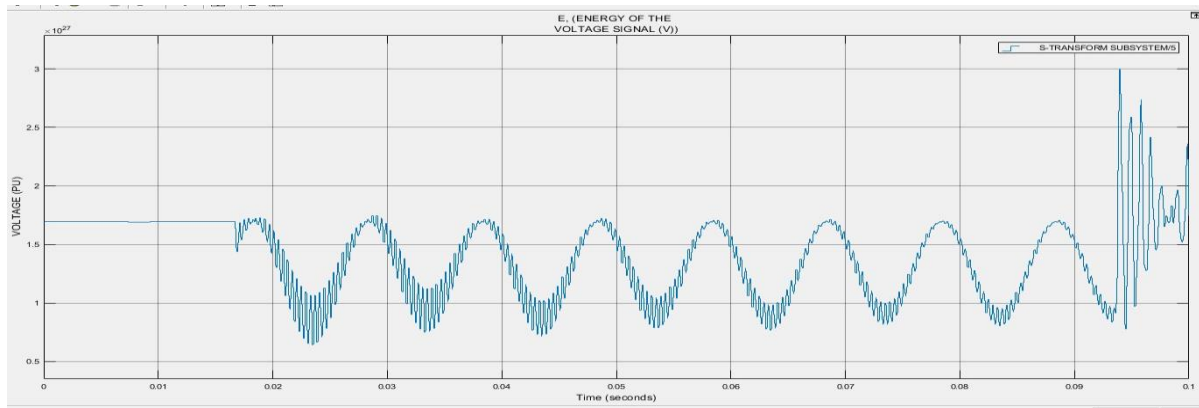


Figure 26: The Voltage Signal Energy Waveform during Phase-to-Phase Fault Condition.

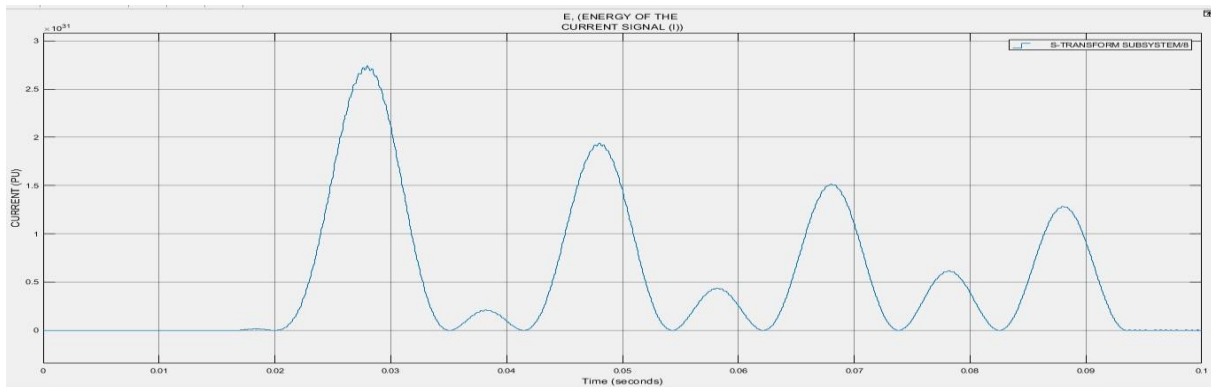


Figure 27: The Current Signal Energy Waveform during Phase-to-Phase Fault Condition.

Figure 28 depicts the fault classification back propagation ANN training process chosen for phase to phase (A-B, B-C, or C-A) fault. It displays the number of iterations (43), the network's performance (0.00767, which is good), and the gradient (0.000805).

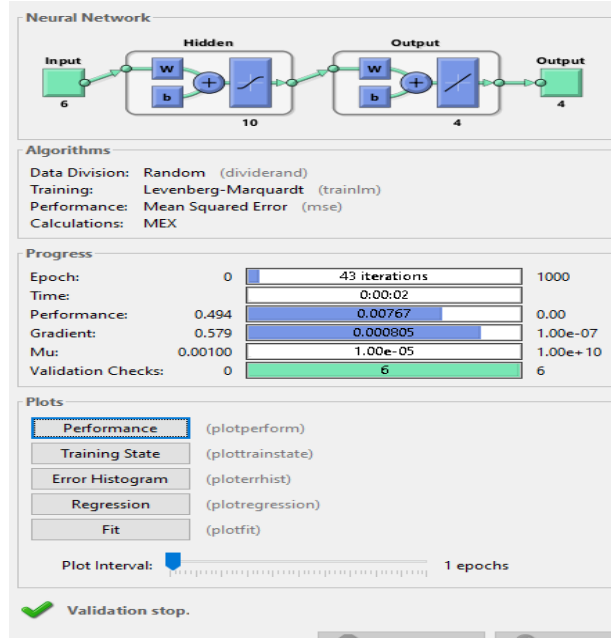


Figure 28: The Fault Classification BP ANN Training Procedure Selected for Phase-to-Phase Fault.

The distance at which the phase-to-phase fault occurred is locate at 44.2km gotten from the output of the traveling wave model.

Table 6: The Result Obtained at Phase-to-Phase Fault Condition

S/N	PARAMETER	MAGNITUDE (PU)
1	Voltage (V)	0.5
2	Current (I)	120
3	Energy of the voltage signal E_j (J)	1.7×10^{27}
4	Energy of the current signal E_j (J)	2.7×10^{31}
5	Mean Square Error (MSE)	0.00767
6	Gradient & Validation	0.000805
7	Fault Distance in km	44.2

iv. At Double Phase to Ground Fault Condition

The following data were obtained when a double phase to ground fault was begun on the system, at a time of 17msecs and persisted until it was cleared at 94msecs, which lasted roughly 77msecs.

The current waveform reveals that once the fault occurs, the faulty phase current magnitudes increase to 120pu for the double phase to ground fault and continue in this manner until the fault is removed. During the fault period, the amplitude of the current flowing through the healthy phase remained constant. After the fault is resolved, the amplitude of the current in the faulty phases becomes uniform with the size of the current in the remaining healthy phase. Figure 30 illustrates the current waveform.

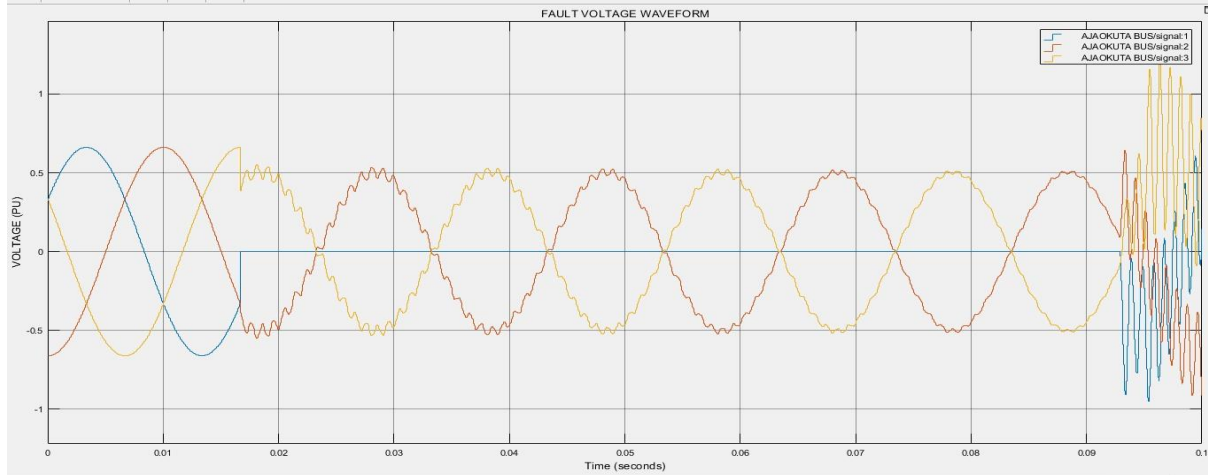


Figure 29: Double Phase to Ground Fault Voltage Waveform for the System Modelled.

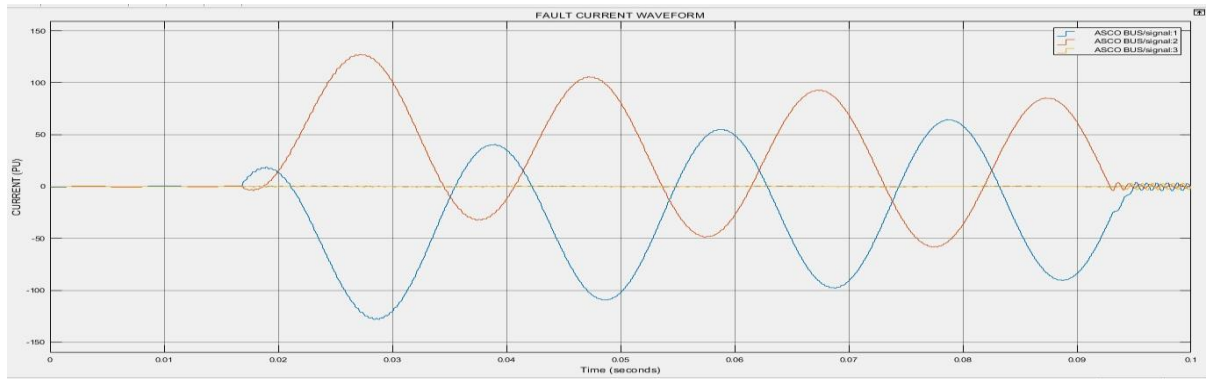


Figure 30: Double Phase to Ground Fault Current Waveform for the System Modelled.

Furthermore, the magnitude of the voltage energy signal from the S-Transform model in Figure 31 gets distorted at $1.7 \times 10^{27} J$ during the fault condition, which is now smaller than the size of the current energy signal in Figure 32 at $2.7 \times 10^{31} J$. When the fault occurs at 17msecs, the current energy signal magnitude spikes to $2.7 \times 10^{31} J$ and is recovered once the fault is cleared at 94msecs.

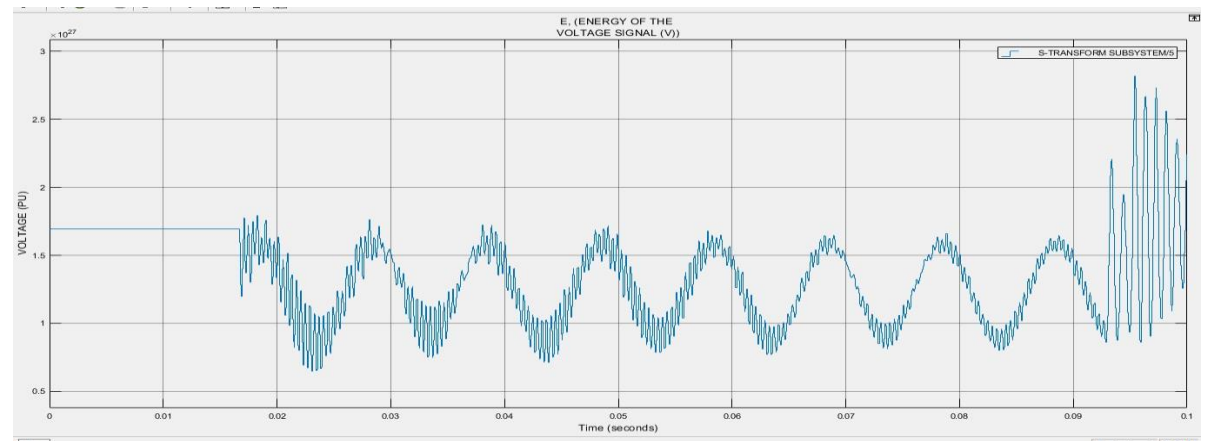


Figure 31: The Voltage Signal Energy Waveform during Double Phase-to- Ground Fault Condition.

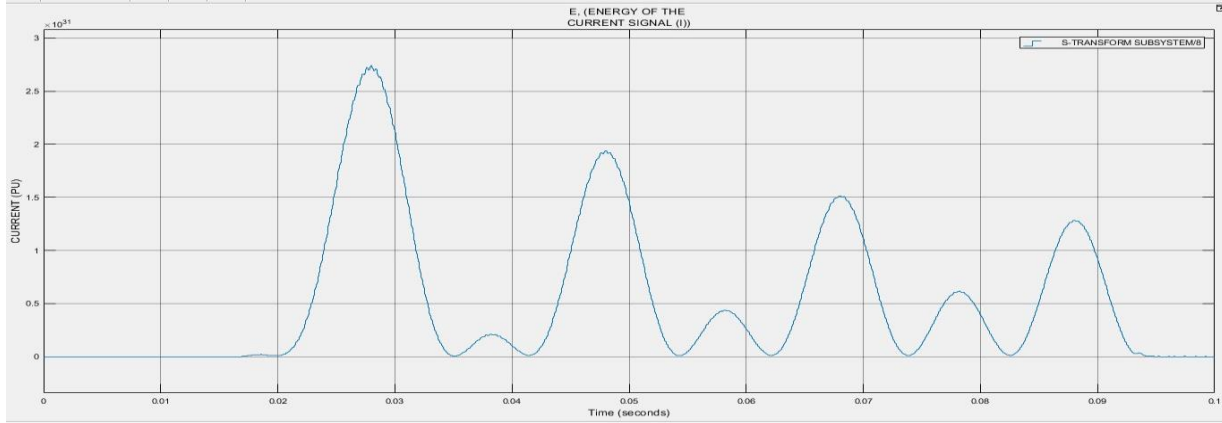


Figure 32: The Current Signal Energy Waveform during Double Phase-to-Ground Fault Condition.

Figure 33 depicts the fault classification back propagation ANN training process chosen for a double phase-to-ground fault. It displays the number of iterations (54), the network's performance (0.00553, which is good), and the gradient (0.00101).

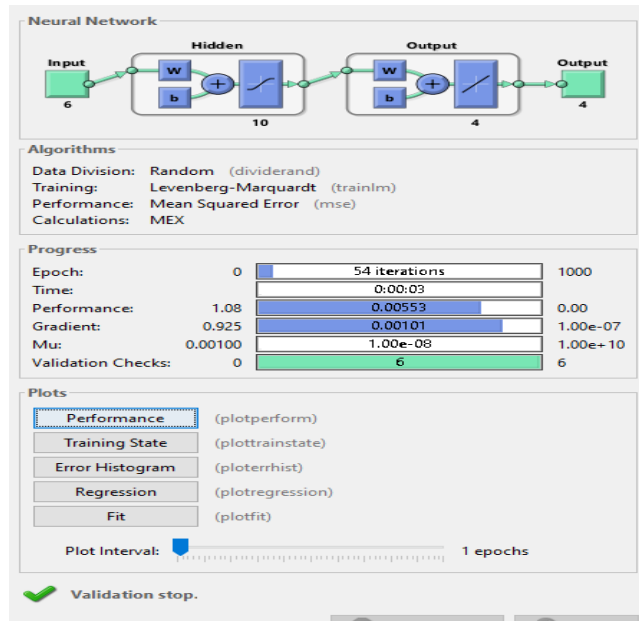


Figure 33: The Fault Classification BP ANN Training Procedure Selected for Double Phase to Ground Fault.

The distance at which the double phase ground fault occurred is locate at 44.74km gotten from the output of the traveling wave model.

Table 7: The Result Obtained at Double Phase to Ground Fault Condition.

S/N	PARAMETER	MAGNITUDE (PU)
1	Voltage (V)	0.5
2	Current (I)	120
3	Energy of the voltage signal E_j (J)	1.7×10^{27}
4	Energy of the current signal E_j (J)	2.7×10^{31}
5	Mean Square Error (MSE)	0.00553
6	Gradient & Validation	0.00101

v. At Three Phase Fault Condition

On simulation of a three-phase fault condition. Figure 34 depicts the voltage waveform. When the fault was triggered, the three-phase voltage dropped from 0.6 to zero at 17msecs and persisted until the fault was cleared at 85msecs before it was restored. This lasted 68 milliseconds. When the three-phase fault was initiated at 17msecs, the current value rose to roughly 130pu for phase A, 150pu for phase B, and 130pu for phase C. This pattern continued until the fault was cleared at 90ms and the current waveform reverted to its initial point of zero. This is clearly seen in Figure 35.

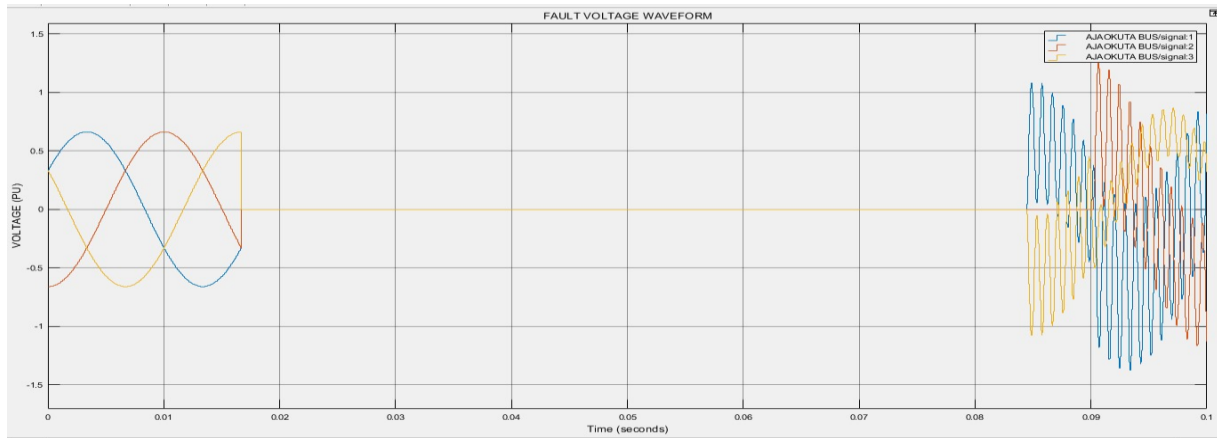


Figure 34: Three Phase Fault Voltage Waveform for the System Modelled.

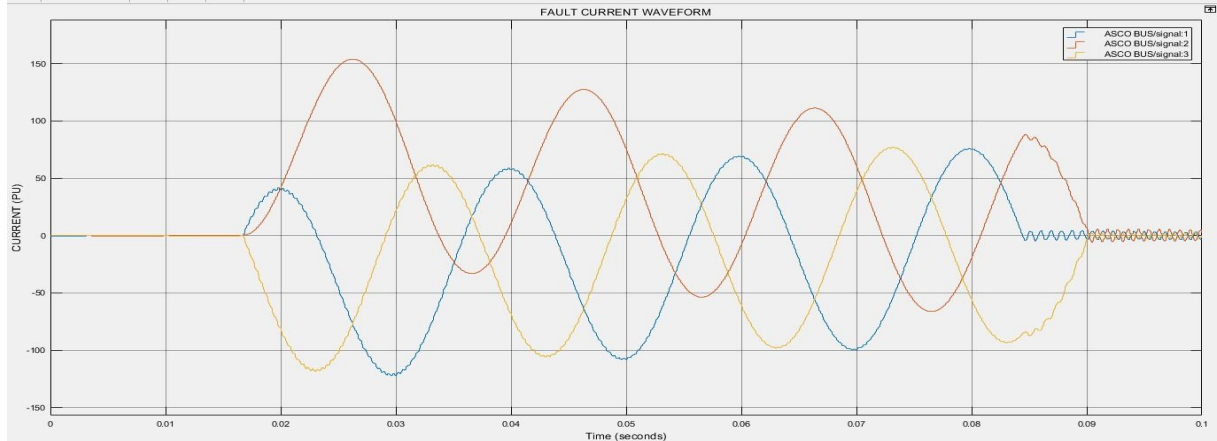


Figure 35: Three Phase Fault Current Waveform for the System Modelled.

Furthermore, the magnitude of the voltage energy signal from the S-Transform model in Figure 36 gets distorted and lowers to $1.7 \times 10^{27} J$ during the fault scenario, which is now smaller than the magnitude of the current energy signal in Figure 37, which is $3.1 \times 10^{31} J$. When the fault occurs at 17msecs, the current energy signal magnitude spikes to $3.1 \times 10^{31} J$ and is recovered once the fault is cleared at 90msecs.

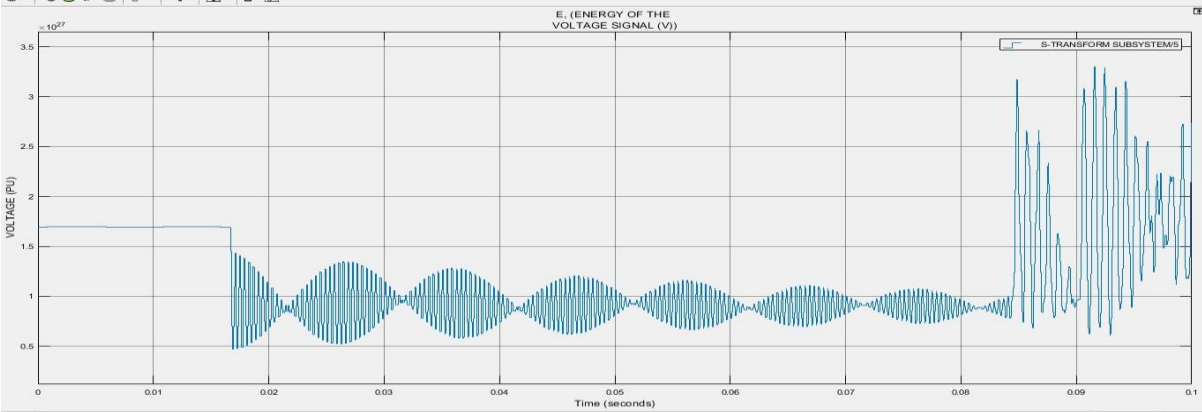


Figure 36: The Voltage Signal Energy Waveform during Three Phase Fault Condition.

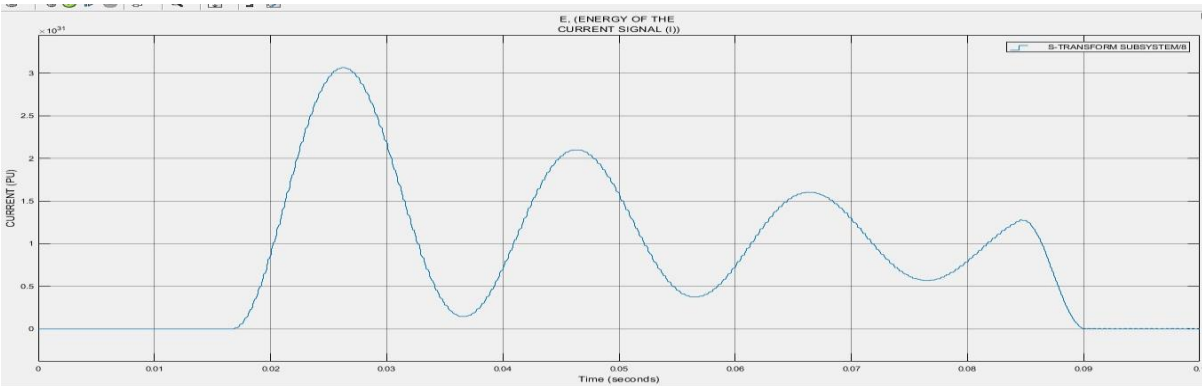


Figure 37: The Current Signal Energy Waveform during Three Phase Fault Condition.

Figure 38 depicts the fault classification back propagation ANN training approach chosen for the three-phase ABC fault. It displays the number of iterations (384), the network's performance (0.00444, which is good), and the gradient (0.00125).

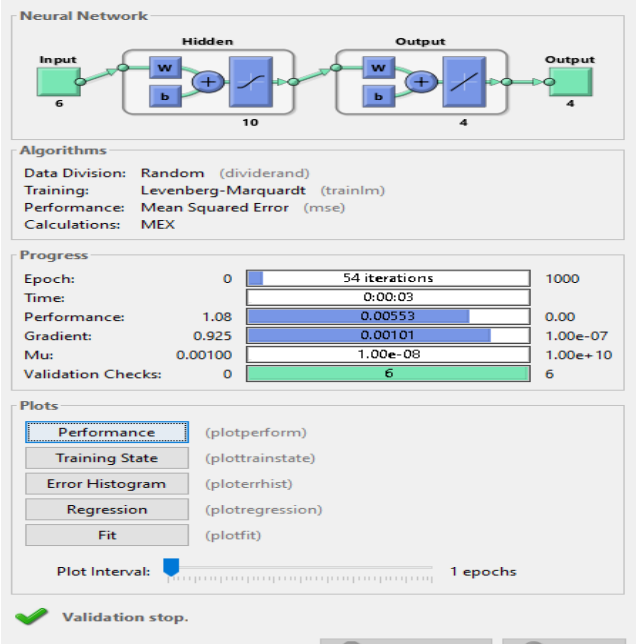


Figure 38: The Fault Classification BP ANN Training Procedure Selected for Three Phase Fault.

The distance at which the three-phase fault occurred is located at 44.76km gotten from the output of the traveling wave model.

Table 8: The Result Obtained at Three Phase Fault Condition

S/N	PARAMETER	MAGNITUDE (PU)
1	Voltage (V)	0.65
2	Current (Ia)	130
3	Current (Ib)	150
4	Current (Ic)	130
5	Energy of the voltage signal E_j (J)	1.7×10^{27}
6	Energy of the current signal E_j (J)	3.1×10^{31}
7	Mean Square Error (MSE)	0.00553
8	Gradient & Validation	0.00101
9	Fault Distance in km	44.76

4.0. Conclusion

This study presents fault diagnosis on a 330kv power system transmission line using integrated s-transform, artificial neural network and travelling wave technique. This paper addressed the issue of service continuity in an electrical power network. The goal of this study was to offer an automated system for fault detection based on S-Transform, pattern recognition of ANN for fault classification, and traveling wave for fault localization on the transmission line. The strategies were evaluated in MATLAB/SIMULINK using data collected by running various fault conditions in the 47.39km Ajaokuta to Lokoja 330kV 58-Bus transmission system model.

The S-Transform was able to display the fault's waveform with a clear changing Gaussian window of the energy signal. At pre-fault condition, the energy of the voltage signal was $1.6947 \times 10^{27} J$ greater than the energy of the current signal at $1.2725 \times 10^{26} J$. While after fault condition say single phase to ground fault, the magnitude of the current signal at $2.0 \times 10^{30} J$ becomes greater than that of the voltage signal at $1.7 \times 10^{27} J$ which are in accordance with conventional circuit theorem. The ANN does not require the line impedance to be calculated, but employs the phase voltages and currents per unit values. In a short period of time, it produces an accurate result by processing large amount data and training it. After 687 iterations, the gradient was at 8.59×10^7 and the best validation performance was 0.609 at 687 epochs. Been self-explanatory, simple and accurate, the neural network was chosen as the best technique fault classification and analysis which successfully classified all fault say single phase to ground at a gradient and validation of 0.00184 and mean square error of 0.0385. The traveling wave approach uses the distance of the line, capacitance of the line, inductance of the line, and propagation velocity to determine the location of the fault say single phase to ground at 44.03km.

This research has been able to present an integral approach to fault diagnosis for grid operators which will improve monitoring of voltages and current signals in-order to detect, classify and locate a fault along the transmission line. This will improve the overall reliability and dependability of the transmission line system and significantly reduces power grid collapse.

References

- Altare, A.S. 2015. Design of a new digital relay for transmission line fault detection, classification and localization based on a new composite relay and artificial neural network approach. Western Michigan University. Retrieved from <https://scholarworks.wmich.edu/masters-thesis/652> on 08 March, 2022.
- Anazia, E.A., Ogbob V.C. and Anionovo, U.E., 2020. Time-frequency analysis technique for fault investigation on power system transmission lines. International journal of engineering inventions, e-ISSN: 2278-7461, p-ISSN: 2319-6491. Volume 9, issue 6, PP: 18-25, 21 August, 2020.

- Hasheminejad, S., Seifassadat, S.G., Razaz, M. and Joorabian, M. 2016. Traveling-wave- based protection of parallel transmission lines using Teager energy operator and fuzzy systems. IET generation, transmission and distribution, 10(4), 1067-1074. Doi: 10.1049/iet-gtd.2015.094, 10 March, 2022.
- Iwuamadi, O.C., Ezechukwu, O.A. and Ogboh, V.C. 2022. Application of S-Transform for fault studies on 330kV transmission line. American journal of engineering research (AJER), 11(01), 75-98. Retrieved from www.ajer.org on 27 March, 2023.
- John, A.A., Obi, K.O. and Anionovo, E.U. 2020. Location of fault on transmission line using traveling wave technique. European journal of energy research, 2(5), 2736-5506. Doi: 10.24018/ejenergy.2022.2.5.90, 27 March, 2023.
- Jose, J.C., Marjan, P., David, L., Sadegh, A. and Vladimir, T. 2021. S-Transform based fault detection algorithm for enhancing distance protection performance. International journal of electrical power and energy systems, 130, 1-9. Doi: 10.1016/j.ijepes.2021.106966, 14 March, 2022.
- Lopes, F.V., Dantas, K.M., Silva, K.M. and Costa, F.B. 2017. Accurate two-terminal transmission line fault location using traveling waves. IEEE transmission power delivery, 33(2), 873-880. Doi: 10.1109/TPWRD.2017.2711262, 10 March, 2022.
- Luke, J. and Erika, G. 2020. Basic of an electrical power transmission system. Retrieved from <https://www.power-and-beyond.com/basic-of-an-electrical-power-transmission-system-a-919739> on 20 December, 2021.
- Majid, J., Sanjeer, K.S. and Rajveer, J. 2015. Fault detection and classification in electrical power transmission system using artificial neural network. Springer Plus, 4, 334. Doi: 10.1186/340064-015-1080-x, 08 March, 2022
- Moursalou. 2015. Power system. Retrieved from <https://circuitglobe.com/power-system.html> on 26 February, 2022.
- Ogboh, V.C., Obute, K.C. and Eleanya, M.N. 2019. Fault classification on power system transmission line using pattern recognition algorithm. International journal of innovative research and advanced studies (IJIRAS), 6(3), 2394-4404. Retrieved from www.ijiras.com/2019/vol_6_issue_3/paper_8.pdf on 27 March, 2023.
- Ogboh, V.C., Nwangugu, E.C. and Anyalebechi, A.E. 2019. Fault detection on power system transmission line using artificial neural network (A comparative case study of Onitsha-Awka-Enugu transmission line). American journal of engineering research (AJER), 8(4), 32-57. Retrieved from www.ajer.org on 08 June, 2023.
- Ravi, K., Ebha, K., Anamika, Y. and Thoke, A.S. 2014. Fault classification of phase-to-phase fault in six phase transmission line using Haar wavelet and ANN. International conference on signal processing and integrated network (SPIN), 5-8. Doi: 10.1109/SPIN.2014.6776911, 07 March, 2022.
- Raza, A., Benrabah, A., Alquthami, T. and Akmal, M. 2020. A review of fault diagnosing methods in power transmission systems. Applied science, 10(4), 1312. Doi: 10.3990/app10041312, 04 March, 2022.
- Shafiullah, M., Abido, M. and Al-Mohammed, A., 2022. Advanced signal processing techniques for feature extraction. Power system fault diagnosis. Pp. 101-120. Doi: 10.1016/B978-0-323-88429-7-00001-1, January, 2022.
- Shafiullah, M. 2024. Fault diagnosis in distribution grids under load and renewable energy uncertainties. Retrieved from https://www.researchgate.net/publication/359931773_Fault_Diagnosis_in_Distribution_Grids_under_Load_and_Renewable_Energy_Uncertainties. On 22 January, 2024.
- Stockwell, R.G., Mansinha, L. and Lowe, R.P. 1996. Localization of the complex spectrum: The S-transform. IEEE transactions on signal processing, 44(4), 998-1001. Doi: 10.1109/78.492555, 13 March, 2022.